TEM and Dual Beam (SEM/FIB) investigations of subsurface cracks and White Etching Area (WEA) formed in a deep groove ball bearing caused by Rolling Contact Fatigue (RCF)

Aleksandro Grabulov[1,2,a] and Henny W. Zandbergen[2]

[1] Netherlands Institute for Metals Research (NIMR), Mekelweg 2, 2600 GA Delft, NL

[2] Delft University of Technology, Kavli Institute of Nanoscience, National Center for HREM Lorentzweg 1, 2628 CJ Delft, The Netherlands

[a] a.grabulov@nimr.nl

Keywords: Rolling Contact Fatigue (RCF), Transmission Electron Microscopy (TEM), Focused Ion Beam (FIB), recrystallisation, subsurface cracks

Abstract. Rolling Contact Fatigue (RCF) is an extreme high-cycle fatigue process (>10^9 load cycles), encountered most often in rolling element bearings and gears. RCF is characterized by very small-scale plastic deformation leading to the formation of so-called butterfly cracks around non-metallic inclusions. This paper presents TEM and Dual Beam (combination of SEM and Focused Ion Beam - FIB), microstructural investigations performed on the subsurface cracks and the White Etching Area (WEA) - butterfly cracks, found in the cross sections of the inner ring of a deep groove ball bearing. Material investigated is hardened and tempered model steel (SAE 52100) containing artificially introduced spherical Al_2O_3 inclusions. The TEM samples for both types of cracks were selected from specific locations using very precise FIB preparation process. TEM investigations show microstructural difference between the WEA (formation of nano-crystalline ferrite) and the steel matrix (tempered martensitic structure). It was found that the formation of the ultra fine ferrite grains was caused by low-temperature recrystallisation process as a result of the crystal point defects stabilization by carbon presence in solid solution.

Introduction

Rolling Contact Fatigue (RCF) can be defined as the mechanism of crack initiation and propagation caused by the near-surface alternating stress field within the rolling contact bodies, which eventually leads to material removal [1]. Contact fatigue is encountered most often in rolling element bearings and gears, where the subsurface shear stresses are high due to the contact stresses under cyclic loading [2]. These stresses are the highest at subsurface stress concentrators (e.g. non metallic inclusions, secondary phases, microstructural defects etc.) or at geometrical imperfections of the contacting surfaces [1].

In this paper we focus on extreme high-cycle RCF process (>10^8 load cycles), involving very small-scale plastic deformation leading to the formation of so-called "butterfly" cracks around stress-raising nonmetallic inclusions. A microstructural characteristic region (~ 5-15μm) of one side of the butterfly crack is called White Etching Area (WEA) or "butterfly wing". It was found by *Sugino* [3] and confirmed by many researchers [3-5] that the WEA form only around oxide, silicate or titanium nitride particles in ordinary ball-bearing steels. They do not form around manganese sulfide or fine carbide particles [4]. Figure 1 represents an SEM image of a butterfly found around an Al_2O_3 inclusion. The butterflies are usually developed on two symmetrical sides of non-metallic inclusion, but they are not always visible in SEM. The specimen preparation process (e.g. cutting angle) can result in cutting off one butterfly wing that lie in different plane. Figure 1 shows that the butterfly wing (WEA) has two distinctive boundaries. One boundary contains the micro crack, propagating from the alumina inclusion, in opposite directions relative to the over-rolling direction. The other boundary does not contain any cracks. The SEM image clearly shows the microstructural difference between WEA and the steel matrix. Those microstructural changes were investigated by means of Transmission Electron Microscope (TEM) and Focused Ion Beam (FIB).

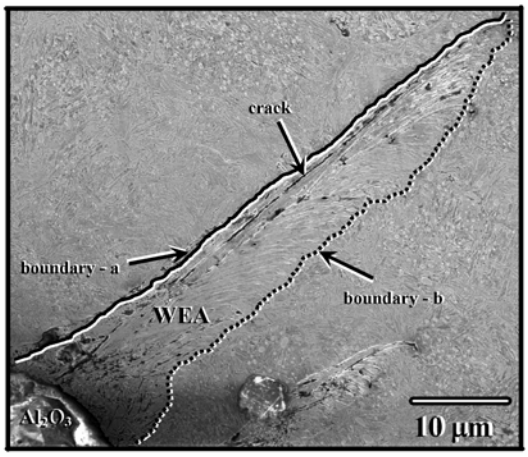

Fig. 1. SEM image of a butterfly crack formed around Al_2O_3 inclusion indicates the White Eatching Area (WEA) "butterfly wing" having two boundaries: one containing a crack, notated as "boundary-a", and the other without a crack notated as "boundary-b". (Longitudinal section with over-rolling from left to right)

Together with the investigations of the subsurface cracks formed in the inner ring of the bearings. Those cracks are found not to be associated with non metallic inclusions. The FIB was used for making the cross sections along the subsurface cracks and the TEM analyses were conducted.

Experimental

The material investigated is a hardened and tempered model steel with a matrix composition similar to the commercial steel grade, SAE 52100. The chemical composition of the steel is given in Table 1.

Table 1. Typical chemical composition of steel SAE 52100 (wt.%)

C	Si	P	S	Cr	Mn
0.97	0.32	0.019	0.017	1.43	0.31

Two types of samples were prepared for this experiment. For the purpose of the butterfly cracks, the investigations were conducted on the model steel containing artificially introduced spherical Al2O3 inclusions. The samples were first austenitized at 860°C and quenched in oil, followed by tempering at 160°C during one hour. The resulting microstructure consists of tempered martensite, retained austenite (10-12 vol-%) and spherical carbides (3-4 vol-%). All samples were exposed to RCF loading using a test rig where two ceramic balls are running in the same track over the circumference of a cylindrical roller having a rotational speed of 15000 rpm, giving a stress cycle frequency of 30 kcpm. The maximum contact stresses were kept at 2.6 GPa, with a total number of stress cycles of 1.3x108. Longitudinal cross sections, parallel to the direction of over-rolling, were made, through the center of the ball running track, followed by metallographic polishing and etching using Nital etchant. The subsurface cracks were investigated from the inner ring (cross section) of the deep groove ball bearing (Fig. 2). The samples prepared for SEM analyses were polishing and Nital etched. In addition all TEM samples from the cross section, contained the cracks were produced by FIB.

TEM Sample Preparation. To be able to correlate TEM images precisely to a location in the butterfly the TEM sample preparation was done with a Focused Ion Beam (FIB), using an FEI Dual Beam DB STRATA 235 system. Figure 3 shows four stages of the FIB preparation process. The first step is marking the exact area of interest (by crosses positioning) and defining the dimension of the lamella (length: 10-15□m and height: 5-7□m).

In this work the lamellas were selected to contain the crack and the microstructure around it. The next step was platinum deposition over the material surface that acts as a protective layer (thickness: 1,5□m), allowing thinning the lamella up to the final thickness without damaging it. The third step was the formation of a staircase through FIB milling on both sides of the lamella using

Ga+ source with a 30kV and the current of 3000pA. The last step involved the final thinning of the lamella (<100nm) using low Ga+ current of 100pA. When the thinning process was completed the lamella was disconnected by FIB from the matrix. Finally, the sample was lifted out and placed on a TEM grid for further analyses.

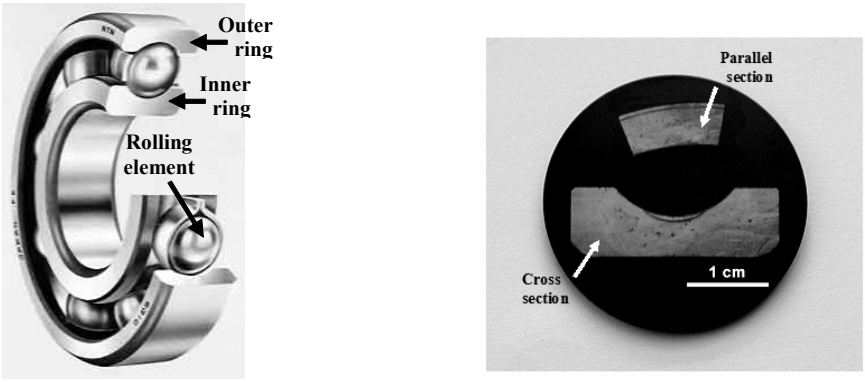

a) b)

Fig. 2. a) Elements of the single row deep groove ball bearing, b) Samples prepared from the inner ring (cross and parallel section)

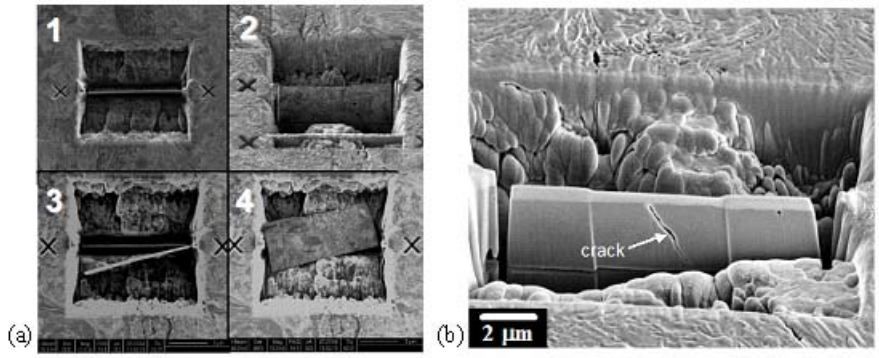

Fig. 3. TEM sample preparation process by FIB: a- (1) positioning and initial milling, (2) additional milling and partial cut of the lamella (3) final cut-off from the material (4) image of the prepared sample prior to the removal, b- FIB image of one lamella containing the crack prepared by FIB

Results and Discussion

SEM Investigations. Figure 1 shows a SEM image of investigated butterfly wing. We observed that all butterfly wings are oriented in the direction of over-rolling and lie at an angle of approximately 45° with respect to the raceway (rolling surface). This fact was previously observed by several researchers, suggesting that the main reason for the orientation of the wings is shear stress that has its maximum value in this direction [5,6]. The cracks extend from the Al_2O_3 particle to the tip of the butterfly wing and form a sharp boundary between the steel matrix and the WEA (Figure 1). The other side of the wing has a feathery, non-smooth boundary in agreement with literature [4]. The origin of the crack is at the contact surface between matrix and the inclusion. Figure 4a shows this interface, being the origin of the cracks. The area marked as "1" represents the place where part of Al_2O_3 was present and removed during the sample preparation process. The area "2" contains large number of microcavities present in the region. The decohesion of inclusion and surrounding matrix causes the nucleation of voids that can lead to the formation of cavities as those visible in Figure 4a [7]. It is likely that under continued straining those cavities grow and coalesce into a central crack which propagates away from the inclusion into the material along localized shear planes at 45° respect to the raceway [8]. This interpretation is strongly supported by previously mentioned observation that butterfly crack lies at the angle of 45° in respect to the over-rolling direction. It is generally accepted that the detrimental effects of the inclusion on the

mechanical properties of the steel are caused by the stress-rising effect or by a weak bonding force at the interface between the inclusion and the surrounding matrix [3]. The residual stress and the stress rising around the inclusion in the combination with the shape of the interface between inclusion and the matrix can result in the formation of multiple cracks and butterfly wings as shown in Figure 4b.

Another observation supported by many WEA studies [3,9] is that spherical carbides normally found in the steel matrix are absent in the butterfly wings. It was also shown [10] the former spherical carbides within WEA, suffer substantial elongations and severe deformation. The shear flow of the carbides located in the WEA is towards the crack and towards the interface between the WEA and the inclusion [1,10,11]. The absence of carbides in the WEA was confirmed also by TEM studies. We can conclude that the carbides must dissolve completely within the WEA.

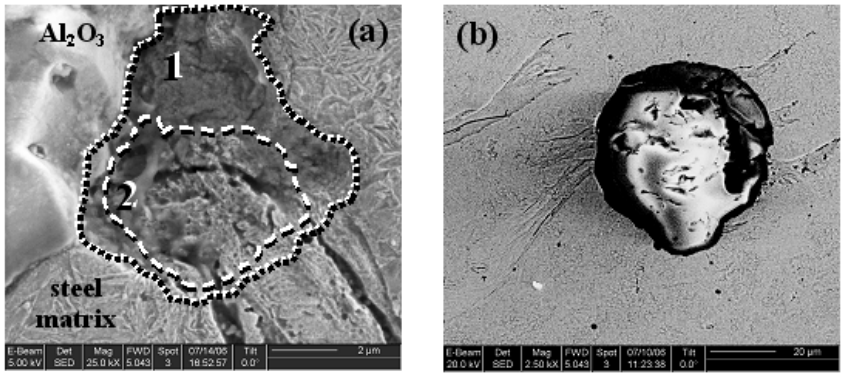

Fig. 4. (a) SEM image of the interface between inclusion and steel matrix. The areas marked as "1" and "2" represent the position where part of Al_2O_3 was located (removed during sample preparation). The area marked as "2", and from which the crack has initiated, shows a large number of microcavities. (b) SEM image illustrating the multi butterflies formation from an alumina inclusion.

TEM Investigations. In order to determine the microstructural differences within the WEA, TEM investigations were carried out. Figure 5 shows one butterfly wing and the locations of TEM samples produced by FIB. This figure also presents the cross section FIB images of TEM lamellas just before their removal. Those images show a clear difference in the microstructure between the steel matrix and White Etching Area. The microstructure also varies within the butterfly wing (WEA) as shown in the cross sections of the lamellas at the locations indicated as 1, 2 and 3 in Figure 5. The size of the grains within WEA gradually decreased in the direction from aluminum oxide towards the tip of the crack (lamella 3 has the smallest grains).

Figure 6a and 6b show TEM images (lamellas 2 and 3 respectively) of the butterfly wing containing the crack and surrounding steel matrix. Large microstructural differences are clearly visible; the steel matrix shows a microstructure of tempered martensite, while the region of butterfly wing (WEA), shows only very fine ferrite grains and no temper carbides. The boundary between those two zones is sharp, indicating that large microstructural changes occurred within WEA. Previous reports [9,12,13] suggested formations of voids in the WEA, and other early observations [4,10,14] reported existence of ferrite grains within WEA. We observed that the main crack was located in the boundary between WEA and the steel matrix and surrounded with secondary micro cracks and voids. We conclude that the formation of secondary micro cracks and voids are the result of high stresses and microstructural changes during RCF (Figure 6a). Further investigations in this study proved that the ultra fine nano-crystalline ferrite grains indeed exist within WEA. Selected Area Diffraction Patterns (SADP) taken from both steel matrix and butterfly wing are shown in Figure 6a. The SADP from steel matrix shows BCC [111] zone axis, while the patterns taken from WEA show rings in diffraction pattern fitting BCC structure of ultra fine nano-crystalline ferrite grains. The ultra-fine ferrite grains vary in size within the WEA. Figure 6a shows few different areas marked as "A" and "B" inside the butterfly wing (WEA). The existence of amorphous-like

regions consisting of very fine ferrite grains are found in areas “A” and larger ferrite grains are distributed along the cracks and between amorphous-like regions (regions “B”). The SADP from both locations (“A” and “B”), clearly indicates difference in the grain size (Figure 6a). Close inspection of the boundary between steel matrix and the WEA, showed the microcracks formed inside the steel matrix, between the martensitic plates, which is in agreement with the previous reports [15] that is a result of the high stresses and deformation present close to the main crack.

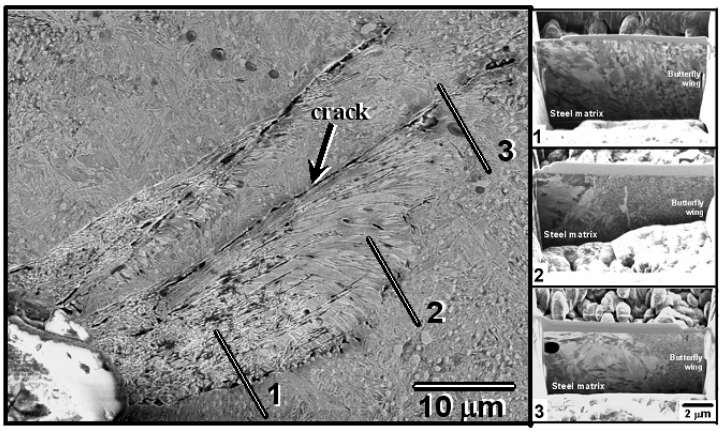

Fig. 5. SEM micrograph showing the butterfly wing and the TEM sample locations. Microstructural difference between the butterfly wing and the steel matrix are clearly visible in the cross sections made by FIB.

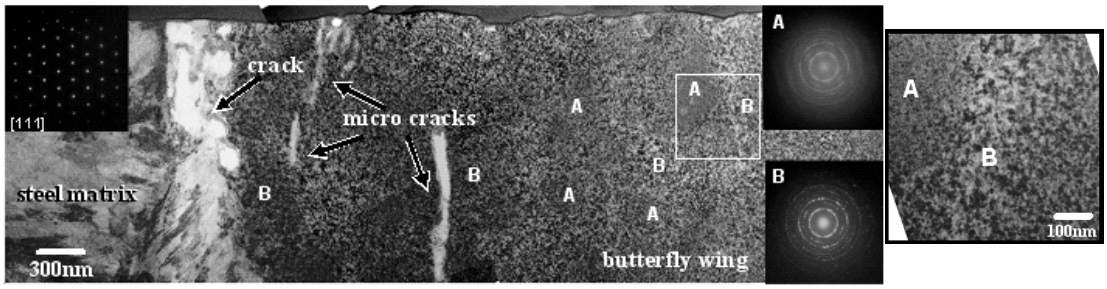

Fig. 6. TEM cross section micrograph of the butterfly wing showing microstructural difference between the WEA and the steel matrix.(a,b represent lamellas 2 and 3 respectively) a) SADP identified the formation of ultra fine nano-crystalline ferrite grain within WEA (“A”: amorphous-like regions, “B”: larger nano-crystalline grains).

We concluded that the observed very fine (nano-sized) ferrite grain structure in the butterfly wings is a result of a recrystallisation process, where new grains form from the highly deformed steel matrix adjacent to the crack faces. This plastic deformation induces high dislocation density, but also high concentrations of crystal point defects. Recrystallisation requires sufficiently high iron self-diffusivity, which normally means thermal activation of vacancy formation and vacancy migration. This translates into the need for a markedly increased operating temperature. In bearing operation, such temperatures can neither be identified as a high steady-state temperature nor as temperature spikes during exposure to the contact stress field. The observed low-temperature recrystallisation effect is here instead interpreted [16] such that the crystal point defects generated during the plastic deformation resulting from the RCF exposure are stabilized by presence of carbon in solid solution [17]. This eliminates the need to thermally activate the formation of vacancies, but only to invoke their mobility to support the recrystallisation process. This is anticipated to readily occur under typical bearing operating conditions.

Subsurface microcracks found in the inner ring of the bearing were investigated using TEM and FIB. The SEM observations of the inner ring cross section (Figure 7a), revealed the formation of subsurface cracks. It was found that the cracks were always parallel to the rolling surface. The size

of the cracks vary from few microns up to 20-30µm, and they are located in depth range of 300-500µm from the rolling surface. The SEM investigations show no evidence of non-metallic inclusion or any defects to be cause of the crack initiation. This could be an indication that these cracks were formed only due to the rolling process and stresses applied during RCF. In order to investigate the microstructure close to the cracks, in-depth observations were performed using series of cross sections made by FIB, which were further investigated by TEM (Figure 7). It was observed that all cracks are oriented approximately 45° with respect to the raceway, as shown in Figure 7b. This proved that the cracks were formed in the direction of the maximal shear stress as previously explained in this paper.

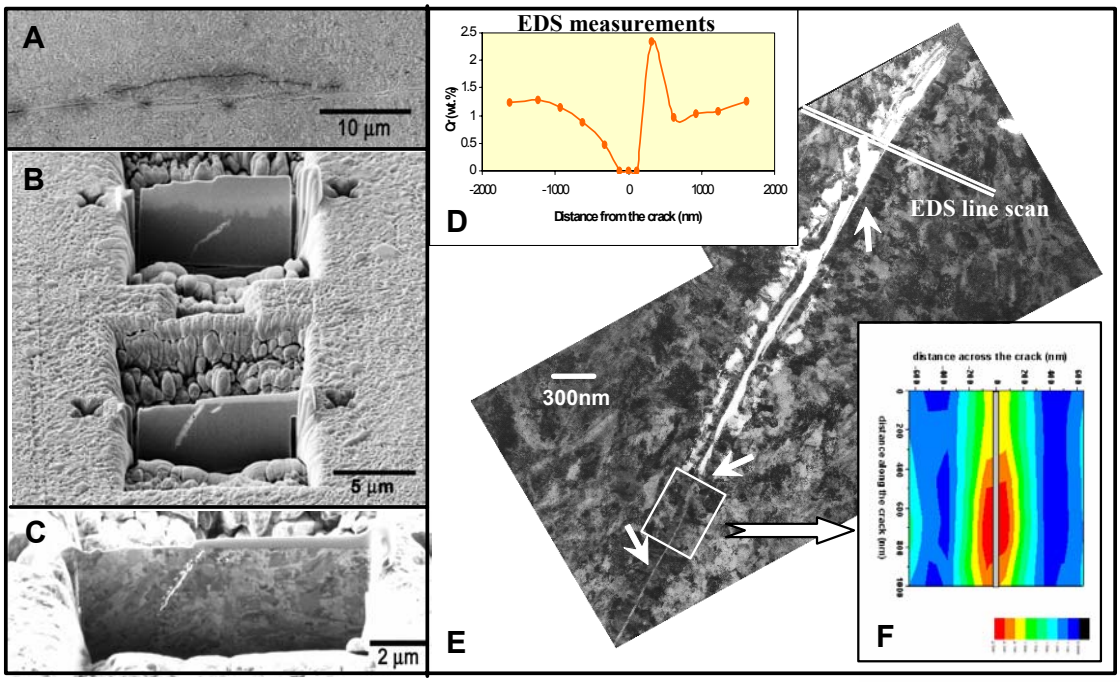

Fig. 7. *A)* SEM image of the subsurface crack, *B)* TEM samples prepared by FIB (lamellas containing the crack), *C)* Lamella prior to final cut, *E)* TEM image of the crack shown in "C", *D)* Diagram presenting EDS measurements (positions marked in "E") of Cr content, *F)* Cr wt% content measured by EDS in area marked in "E".

TEM image of one subsurface crack is presented in Figure 7e. The microstructure of this crack is very different from the cracks observed close to non-metallic inclusions (e.g. butterflies). This suggests that the mechanism of the subsurface crack formation is different from the cracks formed close to non-metallic inclusions. TEM analyses show that the bottom part of the crack is ~ 30nm wide and it gradually opens up to ~ 250nm at the top. In the image one can observe a ~ 50nm wide bands with a darker appearance (indicated in Figure 7e with the arrows). EDS investigations showed a higher concentration of chromium in the bands. Line scans along the cracks from the top of the bottom showed that Cr reaches 2.30 wt.% in average. Figure 7d, represents such a line scan, showing that there is decrease of Cr content on one side of the crack. It was observed that at the other side of the crack Cr content increase rapidly (the layer observed in TEM image) followed by decrease to the minimal value (600nm away from the crack). On the other side of the crack, Cr content is gradually increasing reaching the initial Cr content (~ 1,5 wt%). Figure 7f shows the distribution of Cr from the section of the bottom part of the crack in. The highest concentration of Cr is found in a region close to the crack, decrease further away form the crack and finally stabilizing at the initial Cr content.

Conclusion

In summary, our work provides the explanations of crack initiation and the formation of the ultra fine ferrite grains caused by recrystallisation process. It was shown that the low-temperature recrystallisation occurs as a result of the crystal point defects stabilization by carbon presence in solid solution. Therefore thermal activation is eliminated but only invokes their mobility to support the recrystallisation process. Subsurface cracks were found in the cross section of the inner ring. TEM investigations revealed Cr reach bands formed in the region along the cracks. It was concluded that the cracks were formed as a result of stresses applied and they were not initiated by non metallic inclusions.

Acknowledgement

Authors would like to acknowledge Jan Slycke and Erik Vegter from SKF Engineering Research Centre, Nieuwegein, The Netherlands, for their support and valuable suggestions.
This research was carried out under project number MC5.02127 in the framework of the Strategic Research programme of the Netherlands Institute for Metals Research in the Netherlands (www.nimr.nl).

References

[1] N.P.Suh, An overwiev of the Delamination Theory of Wear, Wear, 44, (1977), 1-16
[2] R.S.Hyde, Rolling Contact of Hardened Steel, (ASM Handbook, 1996) vol. 19, 691-703
[3] K.Sugino, K.Miyamoto, M Nagumo, K Aoki, Transactions ISIJ, 10 (1970), 98-111
[4] P.C.Becker, Metals Technology, Vol 8, (1981), 234-243
[5] J.A.Martin, S.F.Borgese, A.D.Eberhardt, Journal of Basic Engineering, (1966) 555
[6] E.Romhanji, Mehanika i metalurgija deformacije metala, (Beograd: TMF, 2001), 55-77
[7] S.Suresh, Fatigue of Metals, (Cambridge: Cambridge University Press 1991), 122, 388
[8] G.E.Deiter, Mechanical Metallurgy, (London: McGraw-Hill, 1986) 240-271
[9] A.Voskamp, "Microstructural Changes During RCF" (PhD thesis, TU Delft, 1996), 44-83
[10] A.Grabulov, U.Ziese, H.W.Zandbergen, Scripta Materialia 57 (2007) 635-638
[11] H.Schlicht, E.Schreiber, Q.Zwirlein, (ASTM Handbook, 1988), 81-101
[12] H.Harada, T.Mikami, M.Shibata, D.Sokai, A.Yamamoto, H.Tsubakino, ISIJ International, 45 (2005), 1897
[13] M.Nagumo, K.Sugino, K.Aoki, K.Okamoto, Fracture, (1969), 587-597
[14] T.A.Harris, Rolling Bearing Analysis, (New York: Wiley, 2001) 835-861
[15] A.Grabulov, U.Ziese, H.W.Zandbergen,Proceedings of VHCF-4 Conference (in press),Ann Arbor,USA 2007
[16] J. Slycke, SKF Engineering Research Centre, Nieuwegein, The Netherlands, Personal communication
[17] C.J. Först, J. Slycke, K.J. Van Vliet and S. Yip, Physical Review Letters, PRL 96, (2006) 175501